Giant Hall resistance in Pt-based ferromagnetic alloys

G. X. Miao[a] and Gang Xiao
Physics Department, Brown University, Providence, Rhode Island 02912

(Received 6 October 2003; accepted 2 April 2004)

We report on the observation of a dramatically increased extraordinary Hall Effect in Pt-based ferromagnetic alloy thin films with varying composition and thickness that were deposited using magnetron sputtering. Hall slope as high as 76.8 $\mu\Omega$ cm/T has been obtained at 110 K and 22.6 $\mu\Omega$ cm/T at 300 K. Excellent sensitivity, linearity, and a small temperature coefficient have been achieved in a particular composition, $Fe_{35}Pt_{65}$, for a film thickness of 10 nm. The optimized Fe–Pt thin films compare favorably with the commonly used semiconductor Hall sensors. © *2004 American Institute of Physics.* [DOI: 10.1063/1.1757645]

The ferromagnetic extraordinary Hall Effect (EHE) results from spin–orbit scattering of electrons at disorder sites (impurities, grain boundaries, interfaces, etc.) as opposed to the Lorentz force responsible for the ordinary Hall Effect. Pt-based alloys that are rich in spin–orbit interaction are natural candidates for the search of large EHE. Previously, our group reported a large EHE in Fe_xPt_{100-x} alloys[1] that has since been confirmed by others.[2] However, there has been a lack of systematic studies of EHE for various Pt based alloys, particularly for very thin films in the nanometer (nm) range. We have investigated the EHE in four A_xPt_{100-x} thin film systems with A = Fe, Co, Ni, and $Co_{90}Fe_{10}$ with varying composition and thickness. Here we report a giant EHE with a Hall slope as high as 76.8 $\mu\Omega$ cm/T at 110 K and 22.6 $\mu\Omega$ cm/T at room temperature. This is large for a transition-metal magnetic alloy at room temperature.[3–11] We find that varying the film thickness is the key to achieving enhanced EHE.

EHE sensors based on magnetic metallic alloys can operate in the GHz frequency,[12] while semiconductor Hall sensors are restricted to MHz operation. Moreover, the EHE sensors can be made as thin as a few nm, nearly impossible with semiconductor Hall sensors because of their higher resistivity. Due to low carrier concentrations, semiconductor Hall sensors usually offer better sensitivity, to as high as 1000 V/A T without resorting to geometrical enhancements.[13–18] The best sensitivity we have obtained with EHE sensors is about 250 V/A T. We believe further enhancement is entirely possible to exceed the sensitivity offered by the semiconductor counterparts. It is also worth noting that metallic EHE sensors have very low temperature coefficients, as will be shown later.

Our metal-based EHE films exhibit good noise properties (40 nT at 100 Hz and 970 nT at 1 Hz). These numbers, though not optimized, compare favorably with semiconductor sensors. In principle the geometrical enhancement commonly utilized in semiconductor devices[13] should also work for the EHE sensors, and should lead to further improvements in the EHE sensitivity. One of the biggest advantages of EHE sensor is its ease of fabrication (a single layer with a one step lift-off lithography process), making it inexpensive to mass fabricate one- or two-dimensional arrays of EHE sensors for data storage and scanning magnetic microscopy applications. In addition, EHE results from asymmetric scatterings of electrons in the majority- and minority-spin bands; therefore it can be used to detect injected spin currents without an external field.

We used magnetron sputtering to deposit the films, with one Pt target and one magnetic target (A). The base vacuum before deposition was below 1×10^{-7} Torr, and the Ar sputtering-gas pressure during growth was kept at 5 mTorr. We rotated a glass substrate between the two sputtering guns, which generated deposition rates between 0.5 and 2/s, carefully calibrated before each deposition. On each passage, the substrate was coated with an ultrathin layer (<5). We achieved a desired composition by precisely controlling the sputtering time on each gun. All substrates were prepatterned with photoresist and a single lift-off step after deposition yields the Hall bars for measurement. We measured transport properties using the standard four-probe method in a magnetic field, taking precaution to eliminate errors from thermoelectric voltage and Hall-probe misalignment. We found that annealing samples at 400 °C always reduced EHE, because annealing tends to reduce magnetic scatterings needed for EHE.

Figure 1 shows the Hall voltage as a function of mag-

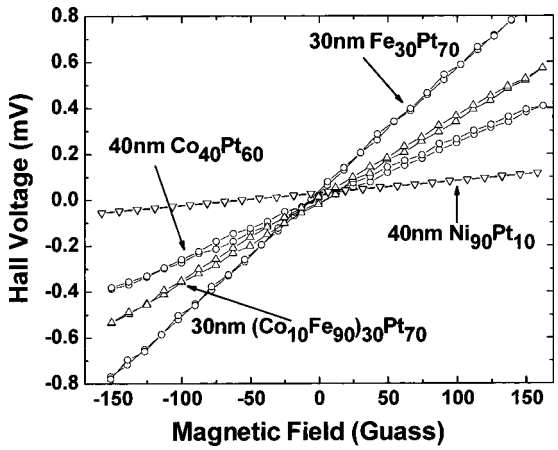

FIG. 1. Hall voltage of some Pt-based alloys vs magnetic field in the low field limit at $T = 300$ K. Excellent linearity is observed. The test current used for the measurement is 5 mA.

[a]Electronic mail: gmaio@us.ibm.com

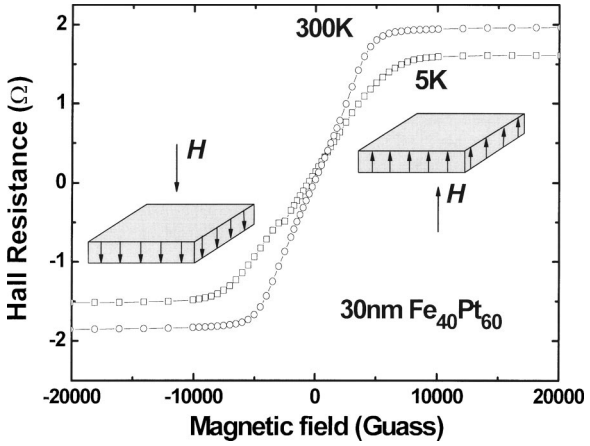

FIG. 2. Hall resistance in a 30 nm thin film $Fe_{40}Pt_{60}$ measured in a broad field range at two different temperatures. Test current is 0.1 mA.

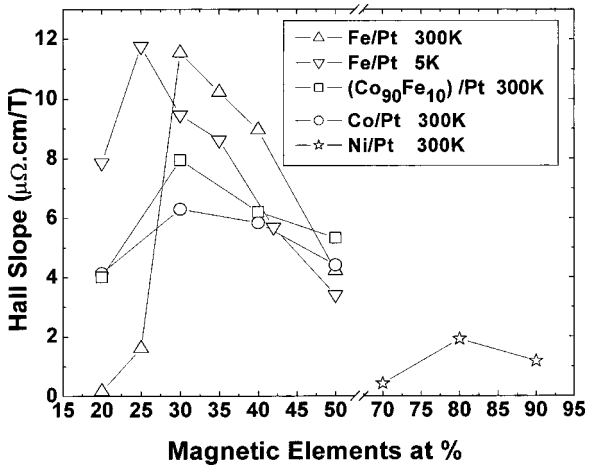

FIG. 3. Initial Hall slope, R_H, vs alloy composition. All the films are 30 nm thick.

netic field measured at $T=300$ K for several alloy films with different compositions. The sensing current used was 5 mA. The result shows that the EHE is nearly perfectly linear as a function of magnetic field, a feature not shared by other sensors, such as those based on giant magnetoresistance or magnetic tunneling.

Figure 2 shows the EHE resistance in a $Fe_{40}Pt_{60}$ (300) film over a broad range of applied field. Under a perpendicular field that is sufficient enough to overcome the shape anisotropy, the magnetization is saturated and so is the EHE. As the magnetization (M) is rotated from the downward to the upward direction, the Hall resistance or the voltage increases linearly with increasing field. The EHE effect is characterized by a parameter called Hall resistivity, expressed as

$$\rho_{xy}=(V_{xy}/I)t=R_0H+4\pi R_sM, \tag{1}$$

where V_{xy} is the Hall voltage, t is the thickness of the film, R_0 is the ordinary Hall coefficient, and R_s is the spontaneous extraordinary Hall coefficient. The term R_0H is several orders-of-magnitude smaller than the term $4\pi R_sM$ for the materials of interest and can be neglected. For a thin film with in-plane magnetic anisotropy, the out-of-plane M increases linearly with field applied in the perpendicular direction until it reaches saturation. Therefore the EHE resistivity is proportional to the perpendicular magnetic field. Above saturation, the Hall resistivity is dominated by the slowly changing OHE. For this reason, the dynamic range is limited by the saturation field of the magnetic film.

For magnetic sensing, the characteristic parameter is the initial Hall slope, defined as

$$R_H=d\rho_{xy}/dH\approx 4\pi\chi R_s, \tag{2}$$

where χ is the constant initial magnetic susceptibility. The quantity R_H is of dual importance. First, it is a direct measure of field sensitivity of an EHE sensor, defined as

$$dV_{xy}/dH=(d\rho_{xy}/dH)jw=R_Hjw. \tag{3}$$

where j is the current density and w is the width of the Hall bar. Second, it is directly related to the physical quantity R_s resulted from spin–orbit interaction as shown in relation (2). We have examined the compositional dependence of EHE in a series of A_xPt_{100-x} films as summarized in Fig. 3, where the initial Hall slopes at 300 K, $R_H=d\rho_{xy}/dH$, are plotted. For comparison, all the samples have the same thickness of 30 nm. Among these samples, $Fe_{30}Pt_{70}$ has the largest Hall slope of 11.8 $\mu\Omega$ cm/T at 300 K. Figure 3 shows that EHE has a peak within a composition range of 25–35 at% of A for all the alloys, except for the Ni_xPt_{100-x} system where the peak occurs at $x=80\%$ and its peak EHE is not as large at those for the other systems. The result in Fig. 3 shows a generic trend. Near the lower composition region (left-hand side of the peak), the reduction in Hall slope is due to two factors: (a) reduced number of magnetic scatterers, and (b) the emergence of paramagnetism at 300 K. In the higher composition region, the decrease of the Hall slope is caused by the gradually increasing saturation field ($H_s=4\pi M$), as M increases with magnetic composition.

Next, we examine the effect of thickness on the EHE. Reduction in the thickness benefits the Hall voltage in two ways. First, according to Eq. (1), $V_{xy}=\rho_{xy}I/t$. Therefore, thinner films yield larger Hall voltage. Second, thinner films tend to have larger resistivity due to enhanced geometrical scattering (ρ-$\rho_{\text{bulk}}\propto 1/t$), which reduces the electron mean-free-path. Figure 4 shows that the Fe/Pt alloy resistivity increases steadily with reducing samples thickness, roughly following a $1/t$ behavior. A larger resistivity also results in a larger EHE resistivity, as $\rho_{xy}\propto\rho\propto\rho_{\text{bulk}}+c/t$ (c is constant)

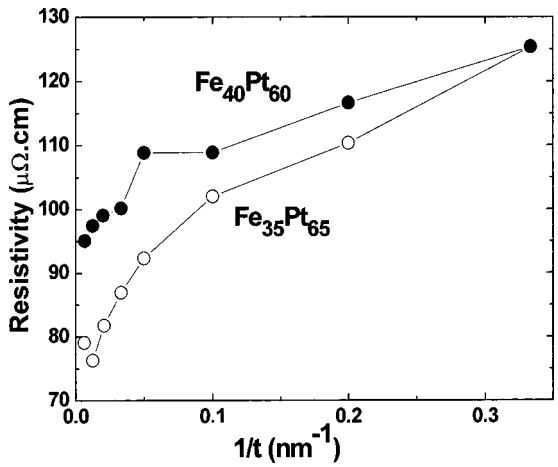

FIG. 4. Inverse thickness dependence of the resistivity at room temperature for two different FePt compositions.

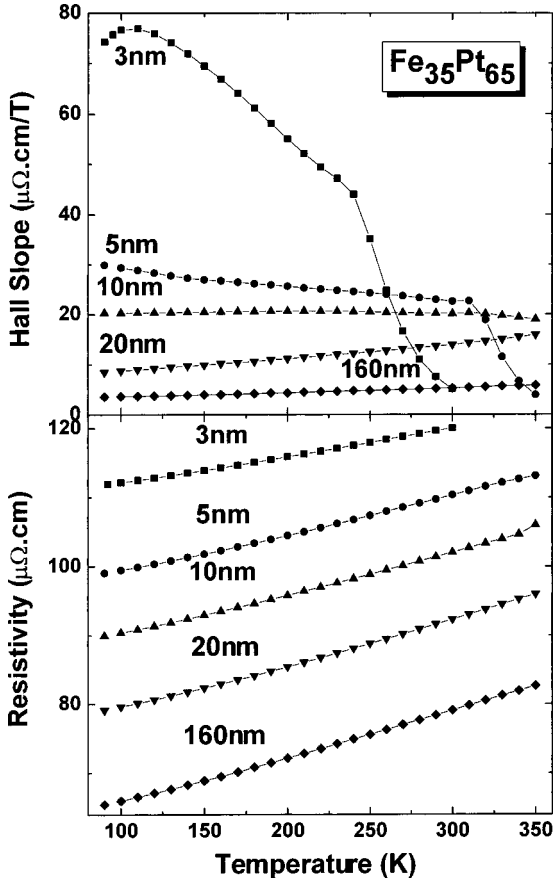

FIG. 5. Hall slope (top) and resistivity (bottom) versus temperature for $Fe_{35}Pt_{65}$ thin films with varying thickness.

for skew scattering and $\rho_{xy} \propto \rho^2 \propto (\rho_{\text{bulk}} + c/t)^2$ for side-jump scattering.[19] For both scattering mechanisms, a reduction in film thickness will result in an increase in the Hall voltage.

Figure 5 shows the effect of thickness on the Hall slope and resistivity of $Fe_{35}Pt_{65}$ between 90 and 350 K. In the thin film limit, the Hall slope and resistivity increase significantly. We have observed a Hall slope as high as 76.8 $\mu\Omega$ cm/T in a 3 nm thin sample at 110 K [Fig. 5(a)]. At 300 K, the 5 nm film has a Hall slope of 22.6 $\mu\Omega$ cm/T. At higher temperatures, the 3 and 5 nm films display a precipitous drop in the Hall effect. This is because these thin films cease to be ferromagnetic near or above 300 K. Interestingly, as the temperature is raised, the Hall slope decreases in the thinner films, but increases in the thicker films. This results in a unique thickness around 10 nm, where a nearly constant Hall slope is obtained between 90 and 350 K. A small temperature coefficient of Hall slope is highly desirable for sensing applications.

In comparison to the GMR ratio commonly used in some magnetic heterostructures, we define the giant Hall resistance ratio as

$$\text{GHR} = (\rho_{xy}\uparrow - \rho_{xy}\downarrow)/\rho_{xx} = (V_{xy}\uparrow - V_{xy}\downarrow)/V_{xx}, \qquad (4)$$

where the arrows referred to the saturated values under fields, assuming that the Hall bar's length equals its width. It should be noted that the GHR can be infinity using the conventional definition of MR since it is a true null detector. According to Eq. (4), $Fe_{35}Pt_{65}$ at 5 nm has a GHR of 7% at room temperature with a saturation field of about 3 kOe. $Fe_{35}Pt_{65}$ at 3 nm has a GHR of 23% at 110 K. Though still lacking the sensitivity of GMR, EHE sensors exhibit excellent linearity and large dynamic range. An EHE sensor is a null detector by itself, whereas GMR sensor requires a bridge circuit for achieving null sensing. All these with the additional benefit of low fabrication cost make Fe/Pt EHE sensors potentially attractive for some applications.

The authors wish to thank Dr. X. X. Zhang and Mr. H. Liu for discussion and assistance in experiments. This work was supported by the National Science Foundation through NSF DMR-0306711 and NSF DMR-0080031.

[1] C. L. Canedy, G. Q. Gong, J. Q. Wang, and G. Xiao, J. Appl. Phys. **79**, 6126 (1996).
[2] M. Wantanabe and T. Masumoto, Thin Solid Films **405**, 92 (2002).
[3] P. Khatua, A. K. Majumdar, A. F. Hebard, and D. Temple, Phys. Rev. B **68**, 144405 (2003).
[4] R. K. Zheng, G. H. Wen, and X. X. Zhang, J. Appl. Phys. **91**, 7424 (2002).
[5] A. Gerber, A. Milner, M. Karpovsky, B. Lemke, H.-U. Habermeier, J. Tuaillon-Combes, M. Negrier, O. Boisron, P. Melinon, and A. Perez, J. Magn. Magn. Mater. **242–245**, 90 (2002).
[6] Y. Kobayashi, K. Honda, Y. Aoki, H. Sato, T. Ono, T. Shinjo, S. A. Makhlof, K. Sumiyama, and K. Suzuki, J. Magn. Magn. Mater. **176**, 164 (1997).
[7] C. K. Lo, I. Klik, C. H. Ho, C. J. Chang, Y. Liou, and Y. D. Yao, IEEE Trans. Magn. **33**, 3526 (1997).
[8] Y. Aoki, K. Honda, H. Sato, Y. Kobayashi, S. Hashimoto, T. Tokoyama, and T. Hanyu, J. Magn. Magn. Mater. **162**, 1 (1996).
[9] V. Korenivski, K. V. Rao, J. Colino, and I. K. Schuller, Phys. Rev. B **53**, R11938 (1996).
[10] R. Morel, L. Abadli, and R. W. Cochrane, J. Appl. Phys. **67**, 5790 (1990).
[11] *The Hall Effect and Its Applications*, edited by C. L. Chien and C. R. Westgate (Plenum, New York, 1980), pp. 158–161.
[12] I. Fergen, K. Seemann, A. v. d. Weth, and A. Schuppen, J. Magn. Magn. Mater. **242–245**, 146 (2002).
[13] J. Heremans, D. L. Partin, C. M. Thrush, and L. Green, Semicond. Sci. Technol. **8**, S424 (1993).
[14] V. Mosser, S. Contreras, S. Aboulhouda, Ph. Lorenzini, F. Kobbi, J. L. Robert, and K. Zekentes, Sens. Actuators, A **43**, 135 (1994).
[15] V. Mosser, S. Aboulhouda, J. Denis, S. Contreras, Ph. Lorenzini, F. Kobbi, and J. L. Robert, Sens. Actuators, A **42**, 450 (1994).
[16] N. Haned and M. Missous, Sens. Actuators, A **102**, 216 (2003).
[17] J. S. Lee, K. H. Ahn, Y. H. Jeong, and D. M. Kim, IEEE Trans. Electron Devices **43**, 1665 (1996).
[18] Y. Sugiyama, H. Soga, and M. Tacano, J. Cryst. Growth **95**, 394 (1989).
[19] J. M. Luttingger, Phys. Rev. **112**, 739 (1958).